Available online at www.sciencedirect.com
ScienceDirect
Ceramics International 37 (2011) 2453–2458
CERAMICS INTERNATIONAL
www.elsevier.com/locate/ceramint

Effects of alumina on the crystallization behavior, densification and dielectric properties of $BaO–ZnO–SrO–CaO–Nd_2O_3–TiO_2–B_2O_3–SiO_2$ glass–ceramics

Hsing-I Hsiang [a,*], Li-Then Mei [a], Shi-Wen Yang [b], Wen-Chang Liao [a], Fu-Su Yen [a]

[a] Department of Resources Engineering, Particulate Materials Research Center, National Cheng Kung University, 70101 Tainan, Taiwan, ROC
[b] Department of Materials Science and Engineering, National United University, Miaoli, Taiwan, ROC

Received 8 September 2010; received in revised form 15 March 2011; accepted 26 March 2011
Available online 26 May 2011

Abstract

The alumina addition effects on the crystallization, sintering behaviors and dielectric properties of $BaO–ZnO–SrO–CaO–Nd_2O_3–TiO_2–B_2O_3–SiO_2$ (Ba–Zn–Sr–Ca–Nd–Ti–B–Si) glass powder were investigated using the differential thermal analyzer (DTA), thermo-mechanical analyzer (TMA), X-ray diffractometer (XRD). The results showed that the addition of alumina powder into Ba–Zn–Sr–Ca–Nd–Ti–B–Si glass changed the crystallization sequence from $Nd_2Ti_4O_{11}–Nd_{0.66}TiO_3$ to $Nd_2Ti_3O_{8.7}–Nd_2Ti_2O_7–Nd_2Ti_4O_{11}$ and increased the densification activation energy due to the dissolution of Al^{3+} ions into the glass structure. Fully densified 30 vol.% alumina-added Ba–Zn–Sr–Ca–Nd–Ti–B–Si glass can be obtained via glass viscous flow before the second and third crystalline phases, $Nd_2Ti_2O_7$ and $Nd_2Ti_4O_{11}$ crystallization. The 30 vol.% alumina-added Ba–Zn–Sr–Ca–Nd–Ti–B–Si glass–ceramics sintered at 900 °C exhibited a high dielectric constant of 17 and a quality factor of about 820, which provided a promising candidate for LTCC applications.

Keywords: A. Sintering; D. Glass ceramic; Crystallization; LTCC

1. Introduction

The microwave telecommunication and satellite broadcasting industries have progressed greatly through portable telephones. The dielectric components must also be miniaturized to reduce the device size. In recent years, low-temperature cofired ceramics (LTCC) have been developed to increase the volume efficiency by integrating passive components such as capacitors, resistors, and inductors [1,2].

LTCC is a ceramic filled glass composite and is based on either the crystallizable glass or a mixture of glass and ceramics [3]. For the LTCC system, the glass mainly acts as a low temperature sintering aid and ceramic fillers help in enhancing mechanical strength and minimizing distortion. High volume content of glass is often detrimental to the quality factor of LTCC materials [4] and hence crystallizable glass + ceramic in which crystallization from glass phase occurs after densification has distinct advantage for LTCC applications. Recently, we investigated the crystallization, sintering behaviors and dielectric properties of $BaO–ZnO–SrO–CaO–Nd_2O_3–TiO_2–B_2O_3–SiO_2$ (Ba–Zn–Sr–Ca–Nd–Ti–B–Si) glass powder and observed that the as-prepared Ba–Zn–Sr–Ca–Nd–Ti–B–Si glass–ceramics sintered at 900 °C exhibited a high dielectric constant of 23 and a quality factor of about 600, which provided a promising candidate for LTCC applications [5,6]. However, the pure glass easily bloats or softens during firing, leading to the distortion of the components and requires the addition of ceramic fillers (such as alumina, cordierite, rutile, etc.) to eliminate softening at 800–900 °C. The alumina powder has been widely used in most of commercial LTCC materials due to cost effectiveness, easy availability with diverse particle sizes and less reactivity with glass [7–9].

Therefore, this study investigated the effects of alumina addition on the crystallization, sintering behaviors and dielectric properties of Ba–Zn–Sr–Ca–Nd–Ti–B–Si glass powder. The proposed method promises a new LTCC material with high dielectric constant and high Q, providing candidates for LTCC applications.

* Corresponding author.
E-mail address: hsingi@mail.ncku.edu.tw (H.-I. Hsiang).

0272-8842/$36.00
doi:10.1016/j.ceramint.2011.05.083

2. Experimental procedures

BaO–ZnO–SrO–CaO–Nd_2O_3–TiO_2–B_2O_3–SiO_2 (Ba–Zn–Sr–Ca–Nd–Ti–B–Si) glass with the composition 3.5 mol% CaO, 6 mol% SrO, 20 mol% BaO, 9.5 mol% Nd_2O_3, 20 mol% ZnO, 24 mol% TiO_2, 5 mol% B_2O_3, 12 mol% SiO_2 was prepared by melting powders containing appropriate amounts of reagent grade $CaCO_3$, $SrCO_3$, $BaCO_3$, Nd_2O_3, ZnO, TiO_2, H_3BO_3, and SiO_2 in a Pt crucible at 1550 °C for 6 h. The melt was rapidly quenched in distilled water, and then ball milled with acetone using 3 mm Y-TZP (yttria-tetragonal zirconia polycrystals) mill media for 12 h. The glass powder had a median size of 4.4 μm. The XRD (Siemens, D5000) analysis did not reveal any crystal phase for the glass powder. The true densities measured using pycnometer (Micromeritics, AccuPyc 1340) for the glass powder was about 4.35 g/cm^3.

The Ba–Zn–Sr–Ca–Nd–Ti–B–Si glass powder was mixed with different amounts of α-alumina powder (AKP-20, Sumitomo Chemical Co.) and then pressed uniaxially at about 300 MPa to make a pellet 8 mm diameter and 2 mm in height. The samples were then sintered at temperatures in the range of 700–950 °C for 1 h. The crystallization behavior and glass transition temperature (T_g) were determined using a differential thermal analyzer (DTA) (Netzsch STA 409C). The DTA was performed at a constant heating rate of 10 °C/min under flowing air. The thermal shrinkage behavior was measured using a thermo-mechanical analyzer (TMA) (Mettler, 840) at a heating rate of 10 °C/min. The crystalline phase evolution was characterized using an X-ray diffractometer with a Cu-Kα (Siemens, D5000). Dielectric properties (relative dielectric constant, Q value) were measured using an LCR meter (YHP 4291A, YHP Co., Ltd.) at 1 MHz.

3. Results and discussion

Fig. 1 shows the DTA measurement result for the Ba–Zn–Sr–Ca–Nd–Ti–B–Si glass added with different amounts of alumina. It was observed that the pure Ba–Zn–Sr–Ca–Nd–Ti–B–Si glass powder exhibits glass transition at around 708 °C, followed by one broadening and one sharp exothermic transformation corresponding to glass crystallization at around 780 °C and 890 °C, respectively. For the samples with added alumina, obscure broadening endothermic and first exothermic peaks occurred in the temperature range between 725 and 790 °C due to glass transition and crystallization, respectively. This was followed by secondary and third exothermic transformations corresponding to glass crystallization at around 850–860 °C and 910–925 °C, respectively. The secondary and third crystallization temperatures were shifted toward lower and higher temperatures, respectively, with an increase with the addition of alumina powder.

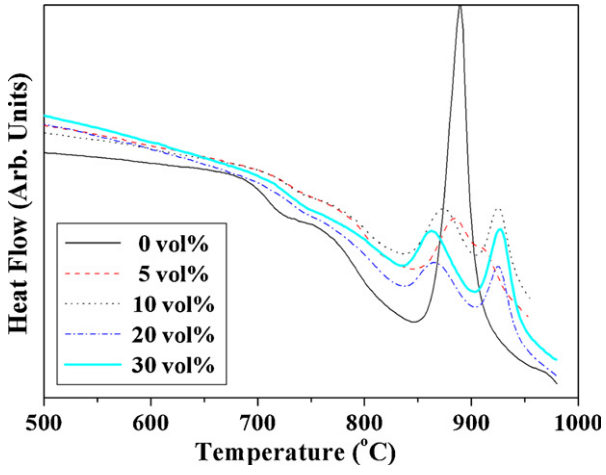

Fig. 1. DTA measurement results for the Ba–Zn–Sr–Ca–Nd–Ti–B–Si glass added with different amounts of alumina.

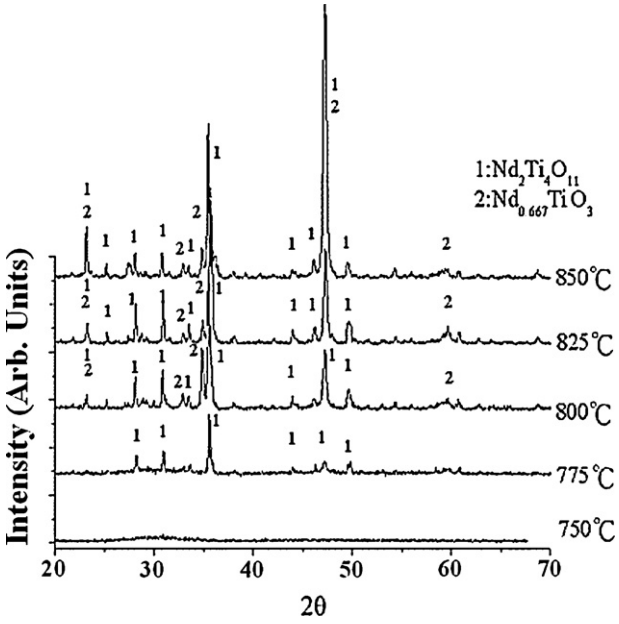

Fig. 2. XRD patterns for the Ba–Zn–Sr–Ca–Nd–Ti–B–Si glass powders sintered at various temperatures for 1 h.

The XRD patterns for the pure Ba–Zn–Sr–Ca–Nd–Ti–B–Si glass powders sintered at various temperatures for 1 h are shown in Fig. 2. The glass sintered at 750 °C was still amorphous. As the sintering temperature was raised to 775 °C, the first crystalline phase, $Nd_2Ti_4O_{11}$ was observed. Therefore, the first broadening exothermic peak in the DTA curve resulted from the crystallization of $Nd_2Ti_4O_{11}$. However, the second crystalline phase, $Nd_{0.667}TiO_3$, occurred at 800 °C, determined from XRD patterns (Fig. 2), lower than the peak temperature for the sharp exothermic peak in the DTA curve. This may be because the XRD patterns were obtained for samples sintered for 1 h, which shifted the $Nd_{0.667}TiO_3$ crystallization temperature to a lower temperature compared with the DTA result. Fig. 3 shows the XRD patterns for the glass added with 30 vol.% alumina powder sintered at various temperatures for 1 h. Fig. 4 shows the variation in the amount of crystalline phases for the glass added with 30 vol.% alumina with the sintering temperature. After sintering at 750 °C, the first crystalline phase, $Nd_2Ti_3O_{8.7}$, was observed accompanied by a small secondary crystalline phase, $Nd_2Ti_2O_7$, with alumina coexistence. Moreover, the XRD peak intensity of the crystalline phase, $Nd_2Ti_3O_{8.7}$ and $Nd_2Ti_2O_7$, increased as the

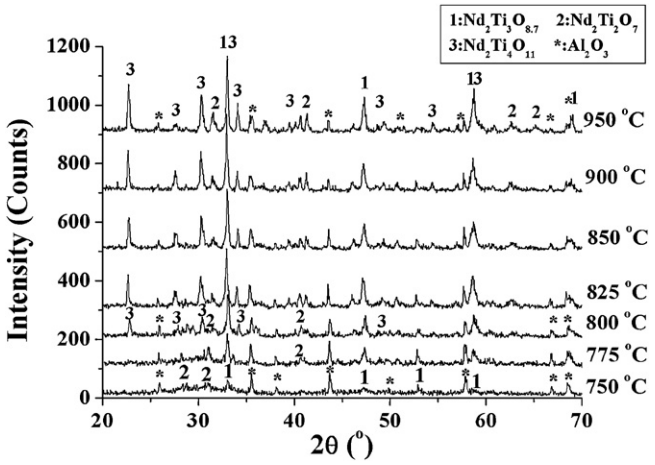

Fig. 3. XRD patterns for the glass added with 30 vol.% alumina powder sintered at various temperatures for 1 h.

sintering temperature was increased from 750 °C to 775 °C and then declined rapidly as the sintering temperature was raised to 800 °C. However, the third crystalline phase, $Nd_2Ti_4O_{11}$, started to occur and increased with decreasing amount of crystalline phase, $Nd_2Ti_3O_{8.7}$ and $Nd_2Ti_2O_7$, in the 775–800 °C temperature region. This implies that the $Nd_2Ti_4O_{11}$ crystalline phase formation may result from the reaction between the crystalline phases, $Nd_2Ti_3O_{8.7}$ and $Nd_2Ti_2O_7$, and residual glass. Note that the XRD intensity of alumina decreased significantly and then remained constant as the sintering temperature was increased from 775 °C to 800 °C, indicating that the alumina may dissolve into the glass network and hence modify the glass structure and viscosity, which influences the glass crystallization behavior during sintering, as shown in Table 1. No crystalline phase other than alumina, $Nd_2Ti_3O_{8.7}$, $Nd_2Ti_2O_7$, and $Nd_2Ti_4O_{11}$ was observed as the sintering temperature was increased above 825 °C. It was found that,

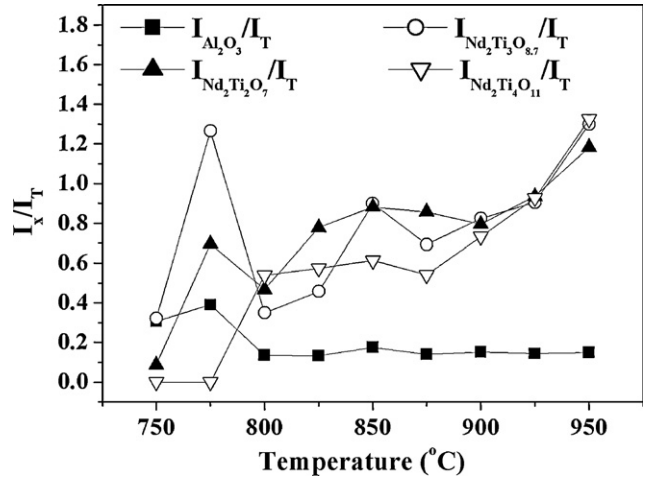

Fig. 4. Variations in the amount of crystalline phases, alumina, $Nd_2Ti_3O_{8.7}$, $Nd_2Ti_2O_7$, and $Nd_2Ti_4O_{11}$ for the glass added with 30 vol.% alumina with the sintering temperature. The amount of crystalline phases for the samples sintered at various temperatures can be semiquantitatively determined by calculating the ratio of the integrated XRD intensities of alumina, $Nd_2Ti_3O_{8.7}$, $Nd_2Ti_2O_7$, and $Nd_2Ti_4O_{11}$ to that of the XRD peak of the internal standard, rutile (I_T).

comparing the DTA and XRD results, the first, second and third exothermic peaks in the DTA curves (Fig. 1) for the glass with added alumina powder can be assigned to the crystallization of $Nd_2Ti_3O_{8.7}$, $Nd_2Ti_2O_7$, and $Nd_2Ti_4O_{11}$, respectively.

The densification behavior is described as densification factor (DF) as a function of time. The DF, which represents the porosity removed during densification, is defined as [10]

$$DF = \frac{D_t - D_g}{D_{th} - D_g}$$

where D_t is the sintered density at time t, D_g is the green density of the as-pressed compact, and D_{th} is the theoretical density calculated using the mixing ratio. The densification behavior for the 30 vol.% alumina-added Ba–Zn–Sr–Ca–Nd–Ti–B–Si glass sintered at temperatures ranging from 725 to 762.5 °C is shown in Fig. 5. The densification factor initially increases rapidly with sintering time, and then less rapidly until it eventually reaches a constant densification factor. A faster and larger densification is observed at a higher temperature. Jean and Lin [11] reported using the kinetic equation derived by Kingery to analyze the liquid phase sintering data and determine the densification mechanism using

$$T\left[\frac{d(DF)}{dt}\right] = K_0 \exp\left(\frac{-Q}{RT}\right)$$

where DF is the densification factor at time t, K_0 is a pre-exponential term, Q is the apparent densification activation energy, R is the gas constant and T is the absolute temperature. Therefore, the apparent activation energy for the rate-controlling step can be determined from the logarithm of the specific densification rate T [d (DF)/dt] versus 1/T for a given densification factor.

The Arrhenius plots of the logarithm of the specific densification rate versus 1/T using the densification data from Fig. 5 at DF = 0.3–0.4, are shown in Fig. 6.

The apparent activation energy determined from the slopes in Fig. 6 using a least-squares-fit method is about 480 ± 13 kJ/mol. The activation energy of the 30 vol.%-alumina-added glass is higher than that of pure glass (305–438 kJ/mol) [5], indicating that alumina powder added into Ba–Zn–Sr–Ca–Nd–Ti–B–Si glass may dissolute into the glass and change the glass structure and increase the viscosity [12], which is consistent with the XRD result (Fig. 4).

Fig. 7 shows the shrinkage behaviors of the powder compacts for the Ba–Zn–Sr–Ca–Nd–Ti–B–Si glass added with different amounts of alumina powder. The onset shrinkage temperature occurred at around 730 °C, which is close to T_g, determined by DTA. The offset shrinkage temperature and linear shrinkage decreased with increasing the addition of alumina. For the samples added with 5, 10, 20, and 30 vol.% alumina, the linear shrinkage are 27, 24, 18, and 18%, respectively, and the shrinkage finished at 850–870 °C, suggesting that full densification can be reached in the temperature range between 850 and 900 °C. However, as the alumina content was increased above 40 vol.%, the linear shrinkage became below 10%, showing that it can not be fully

Table 1
Comparison of the glass crystallization behaviors determined from the XRD and DTA results for the pure glass and 30 vol.% alumina-added glass during sintering.

Sample	First crystalline phase	Second crystalline phase	Third crystalline phase
Pure glass	$Nd_2Ti_4O_{11}$ (T_p: 790 °C)	$Nd_{0.667}TiO_3$ (T_p: 910 °C)	–
30 vol.% alumina-added glass	$Nd_2Ti_3O_{8.7}$ (T_p: 780–790 °C)	$Nd_2Ti_2O_7$ (T_p: 860–870 °C)	$Nd_2Ti_4O_{11}$ (T_p: 925 °C)

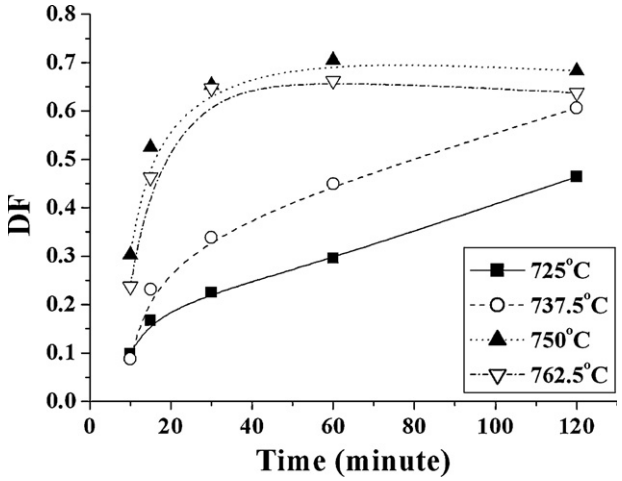

Fig. 5. Densification behavior for the 30 vol.% alumina-added Ba–Zn–Sr–Ca–Nd–Ti–B–Si glass sintered at temperatures ranging from 725 to 762.5 °C.

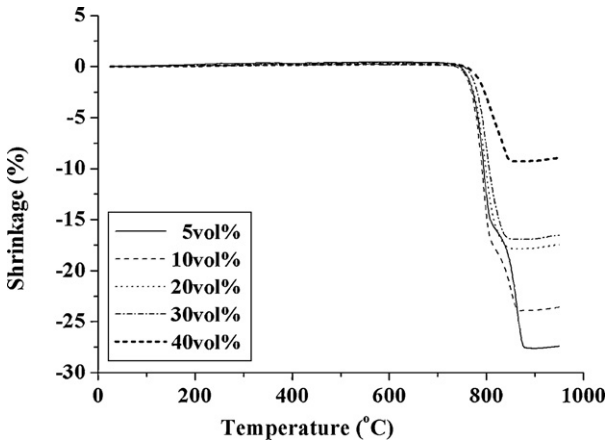

Fig. 7. Shrinkage behaviors of the powder compacts for the Ba–Zn–Sr–Ca–Nd–Ti–B–Si glass added with different amounts of alumina powder (the heating rate was 10 °C/min).

densified below 900 °C. Fig. 8 shows the densification rate of the powder compacts for the Ba–Zn–Sr–Ca–Nd–Ti–B–Si glass added with different amounts of alumina powder as a function of the sintering temperature. The samples added with 5–30 vol.% alumina all exhibited two step shrinkage. The first maximum shrinkage rate occurred at around 800 °C, which is close to the peak temperature of $Nd_2Ti_3O_{8.7}$ crystallization, determined by DTA. This indicates that crystallization would result in densification degradation. In addition, the other saddle points in the curve in Fig. 8 occurred at around 820–860 °C, which is close to the $Nd_2Ti_2O_7$ crystallization temperature, determined by DTA, and were shifted toward lower temperature with an increase in added alumina powder, suggesting that full densification can be obtained via glass viscous flow before the $Nd_2Ti_2O_7$ crystallization. Note that the third crystalline phase, $Nd_2Ti_4O_{11}$, occurred after full densification.

Fig. 9 shows the dielectric properties of Ba–Zn–Sr–Ca–Nd–Ti–B–Si glass added with different amounts of alumina powder as a function of the sintering temperature. The change in dielectric properties is mainly attributed to the variation in density and phase constituents during sintering [13]. The dielectric constant value and Q value increased monotonically with increasing sintering temperature due to the increase in crystalline phase and relative density. In addition, the dielectric

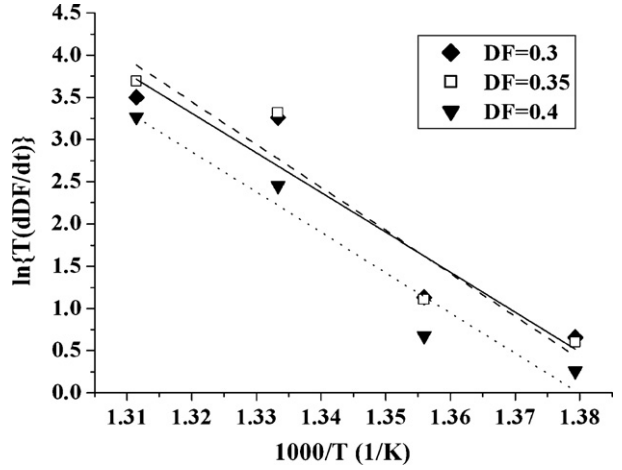

Fig. 6. Logarithm of the specific densification rate $T[d(DF)/dt]$ versus $1/T$ for a given densification factor for the glass added with 30 vol.% alumina at DF = 0.3–0.4.

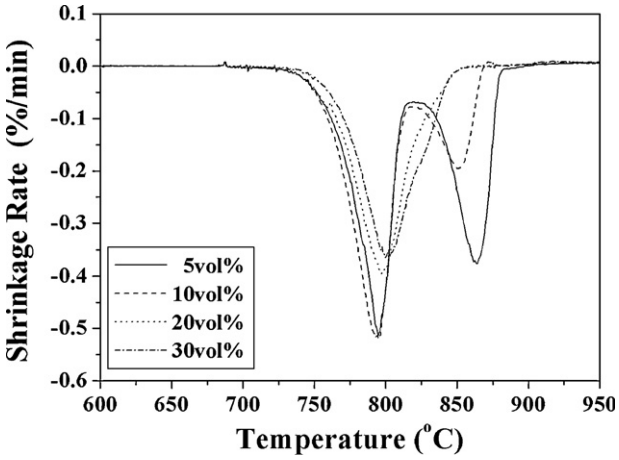

Fig. 8. Densification rate of the powder compacts for the Ba–Zn–Sr–Ca–Nd–Ti–B–Si glass added with different amount of alumina powder as a function of the sintering temperature (the heating rate was 10 °C/min).

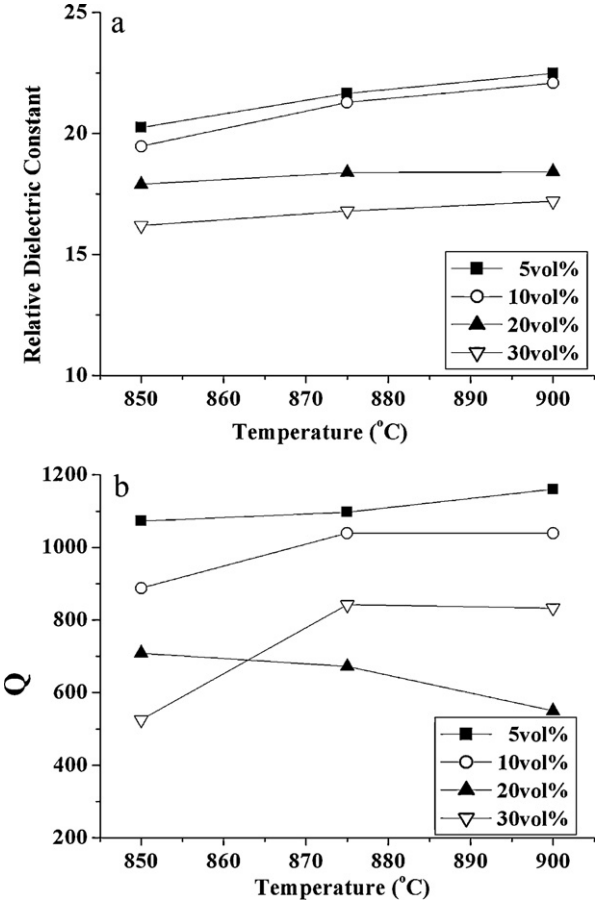

Fig. 9. (a) Relative dielectric constant and (b) Q value of Ba–Zn–Sr–Ca–Nd–Ti–B–Si glass added with different amounts of alumina as a function of the sintering temperature.

constant decreased with the increase in alumina powder, because the dielectric constant of alumina is about 9, which is lower than that of pure Ba–Zn–Sr–Ca–Nd–Ti–B–Si glass (about 23). It is well known that the quality factor is primarily dependent on the network structure of the remnant glass phase and the quality factor decreases with an increase in the amount of residual glass [13]. The amount of crystalline phases ($Nd_2Ti_3O_{8.7}$ + $Nd_2Ti_2O_7$ + $Nd_2Ti_4O_{11}$), for the samples can be semi-quantitatively determined by calculating the ratio of the integrated XRD intensities of $Nd_2Ti_3O_{8.7}$ + $Nd_2Ti_2O_7$ + $Nd_2Ti_4O_{11}$ ($I_1 + I_2 + I_3$) to that of the XRD peak of the internal standard, rutile (I_T). Fig. 10 shows the total amount of crystalline phases ($Nd_2Ti_3O_{8.7}$ + $Nd_2Ti_2O_7$ + $Nd_2Ti_4O_{11}$, $I_1 + I_2 + I_3$) for glass added with different amounts of alumina at 875 °C. Note that the total amount of crystalline phase increased as the alumina content was increased to 30 vol.%. The residual glass decreases with the increase in the total amount of crystalline phases. Therefore, the Q value of the glass added with 30 vol.% alumina powder sintered at 875 °C was higher than that of glass added with 20 vol.% alumina powder. The dielectric properties of the Ba–Zn–Sr–Ca–Nd–Ti–B–Si glass–ceramics added with 30 vol.% alumina powder sintered at 900 °C show a high dielectric constant of 17 and a quality factor of about 820 combined with other (processing,

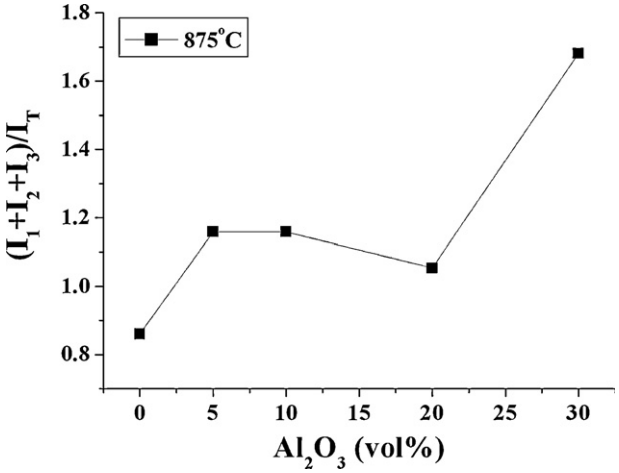

Fig. 10. Total amount of crystalline phases ($Nd_2Ti_3O_{8.7}$ + $Nd_2Ti_2O_7$ + $Nd_2Ti_4O_{11}$, $I_1 + I_2 + I_3$) for glass added with different amounts of alumina at 875 °C. I_1, I_2 and I_3: XRD peak intensities of $Nd_2Ti_3O_{8.7}$, $Nd_2Ti_2O_7$, and $Nd_2Ti_4O_{11}$, respectively; I_T: XRD peak intensity of the internal standard, rutile.

mechanical, thermal electric properties), which provides a promising candidate for LTCC applications.

4. Conclusions

The alumina addition effects on the crystallization, sintering behaviors and dielectric properties of glass–ceramics (BaO–ZnO–SrO–CaO–Nd_2O_3–TiO_2–B_2O_3–SiO_2) were analyzed. The addition of alumina into the glass changed the crystallization behavior and densification activation energy due to the dissolution of Al^{3+} ions into the glass network. This modified the glass structure and viscosity. The full densification of 30 vol.% alumina-added Ba–Zn–Sr–Ca–Nd–Ti–B–Si glass can be obtained via glass viscous flow before the second and third crystalline phase, $Nd_2Ti_2O_7$ and $Nd_2Ti_4O_{11}$, crystallization. The dielectric properties of the Ba–Zn–Sr–Ca–Nd–Ti–B–Si glass–ceramics depend on the total amount of crystalline phases. The dielectric properties of the Ba–Zn–Sr–Ca–Nd–Ti–B–Si glass–ceramics added with 30 vol.% alumina powder sintered at 900 °C showed a high dielectric constant of 17 and a quality factor of about 820, which provides a promising candidate for LTCC applications.

Acknowledgment

This work was financially sponsored by the National Science Council of the Republic of China (98-2221-E-006-077-MY3).

References

[1] A. Baker, M. Lanagan, C. Randall, E. Semouchkina, G. Semouchkin, K.Z. Rajah, R. Eitel, K.Z. Rajab, R. Mittra, S. Rhee, Integration concepts for the fabrication of LTCC structures, Int. J. Appl. Ceram. Technol. 2 (2005) 514–520.

[2] Y.S. Lin, C.C. Liu, K.M. Li, C.H. Chen, Design of an LTCC tri-band transceiver module for GPRS mobile applications, IEEE Trans. Micro Theory Technol. 52 (2004) 2718–2724.

[3] M.T. Sebastian, H. Jantunen, Low loss dielectric materials for LTCC applications: a review, Int. Mater. Rev. 53 (2008) 57–90.
[4] C.J. Dileep Kumar, T.K. Sowmya, E.K. Sunny, N. Raghu, Influence of nature of filler on densification of anorthite-based crystallizable glass1 ceramic system for low temperature cofired ceramics application, J. Am. Ceram. Soc. 92 (2009) 595–600.
[5] H.I. Hsiang, L.T. Mei, W.C. Liao, Fu-Su Yen, Crystallization behavior and dielectric properties of a new high dielectric constant LTCC material based on Nd_2O_3–TiO_2–SiO_2 glass–ceramics, J. Am. Ceram. Soc. 93 (2010) 1714–1717.
[6] Hsing-I. Hsiang, Li-Then Mei, Chi-Shiung Hsi, Wen-Chang Liao, Fu-Su Yen, Crystallization behavior and dielectric properties of BaO–ZnO–SrO–CaO–Nd_2O_3–TiO_2–B_2O_3–SiO_2 glass–ceramics, J. Alloys Compd. 502 (2010) 387–391.
[7] Y.J. Seo, J.H. Jung, Y.S. Cho, Influences of particle size of alumina filler in an LTCC system, J. Am. Ceram. Soc. 90 (2007) 649–652.
[8] J.H. Jean, C.R. Chang, R.L. Chang, T.H. Kuan, Effect of alumina particle size on prevention of crystal growth in low-k silica dielectric composite, Mater. Chem. Phys. 40 (1995) 50–55.
[9] I.J. Choi, Y.S. Cho, Effects of various oxide fillers on physical and dielectric properties of calcium aluminoborosilicate-based dielectrics, J. Electroceram. 23 (2009) 185–190.
[10] J.H. Jean, T.K. Gupta, Densification kinetics and modeling of glass-filled alumina composite, J. Mater. Res. 9 (1994) 771–780.
[11] J.H. Jean, S.C. Lin, Effects of borosilicate glass on densification and properties of borosilicate glass + TiO_2 ceramics, J. Mater. Res. 14 (1999) 1359–1363.
[12] J.H. Jean, Y.C. Fang, S.X. Dai, D.L. Wilcox, Effects of alumina on devitrification kinetics and mechanism of K_2O–CaO–SrO–BaO–B_2O_3–SiO_2 glass, Jpn. J. Appl. Phys. 42 (2003) 4438–4443.
[13] G.H. Chen, X.Y. Liu, Low-temperature-sintering and characterization of glass–ceramic composites, J. Mater. Sci.: Mater. Electron. 17 (2006) 877–882.